

AD-A056 398

MECHANICAL TECHNOLOGY INC LATHAM N Y

F/G 13/9

ROLLING ELEMENT BEARING AND LUBRICANT TECHNOLOGY PROGRAM. PART --ETC(U)

DEC 77 P K GUPTA

F33615-77-C-5100

UNCLASSIFIED

MTI-78TR7

AFML-TR-77-229

NL

1 OF 1
ADA
056398



END
DATE
FILMED

8-78

DDC

AD A056398

AFML-TR-77-229

LEVEL II

(2)

**ROLLING ELEMENT BEARING AND
LUBRICANT TECHNOLOGY PROGRAM**

Part I: Prediction of Torque in DMA Bearings

*MECHANICAL TECHNOLOGY INCORPORATED
968 ALBANY-SHAKER ROAD
LATHAM, NEW YORK 12110*

DECEMBER 1977

TECHNICAL REPORT AFML-TR-77-229
Interim Report March 1977 – September 1977



Approved for public release; distribution unlimited.

AIR FORCE MATERIALS LABORATORY
AIR FORCE WRIGHT AERONAUTICAL LABORATORIES
AIR FORCE SYSTEMS COMMAND
WRIGHT-PATTERSON AIR FORCE BASE, OHIO 45433

78 07 13 027

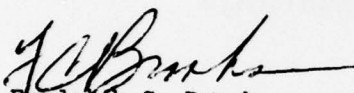
AD No. _____
DDC FILE COPY


NOTICE

When Government drawings, specifications, or other data are used for any purpose other than in connection with a definitely related Government procurement operation, the United States Government thereby incurs no responsibility nor any obligation whatsoever; and the fact that the Government may have formulated, furnished, or in any way supplied the said drawings, specifications, or other data, is not to be regarded by implication or otherwise as in any manner licensing the holder or any other person or corporation, or conveying any rights or permission to manufacture, use, or sell any patented invention that may in any way be related thereto.

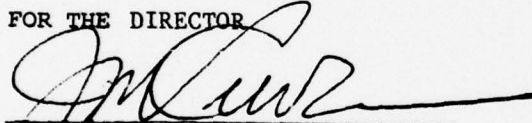
This report has been reviewed by the Information Office (OI) and is releasable to the National Technical Information Service (NTIS). At NTIS, it will be available to the general public, including foreign nations.

This technical report has been reviewed and is approved for publication.


Fredrick C. Brooks
Project Monitor


R. J. BENZING, Chief
Lubricants and Tribology Branch

FOR THE DIRECTOR


J. M. KELBLE, Chief
Nonmetallic Materials Division

Copies of this report should not be returned unless return is required by security considerations, contractual obligations, or notice on a specific document.

Unclassified

SECURITY CLASSIFICATION OF THIS PAGE (When Data Entered)

19 REPORT DOCUMENTATION PAGE		READ INSTRUCTIONS BEFORE COMPLETING FORM	
1. REPORT NUMBER 18 AFML-TR-77-229	2. GOVT ACCESSION NO.	3. RECIPIENT'S CATALOG NUMBER	
4. TITLE (and Subtitle) ROLLING ELEMENT BEARING AND LUBRICANT TECHNOLOGY PROGRAM, PART I, PREDICTION OF TORQUE IN DMA BEARINGS		5. TYPE OF REPORT & PERIOD COVERED Interim Report March 1977 - September 1977	
7. AUTHOR(s) 10 Pradeep K. Gupta		6. PERFORMING ORG. REPORT NUMBER 78TR7	
9. PERFORMING ORGANIZATION NAME AND ADDRESS Mechanical Technology Incorporated 968 Albany-Shaker Road Latham, New York 12110		8. CONTRACT OR GRANT NUMBER(s) 15 F33615-77-C-5100 2W	
11. CONTROLLING OFFICE NAME AND ADDRESS Air Force Materials Laboratory (MBT) Wright Patterson Air Force Base, Ohio 45433		10. PROGRAM ELEMENT, PROJECT, TASK AREA & WORK UNIT NUMBERS 16 2421-02-02 17 P2	
14. MONITORING AGENCY NAME & ADDRESS (if different from Controlling Office) 14 MTI-78TR7		12. REPORT DATE 17 December 1977	
		13. NUMBER OF PAGES 44 18 47	
		15. SECURITY CLASS. (of this report) Unclassified	
		15a. DECLASSIFICATION DOWNGRADING SCHEDULE	
16. DISTRIBUTION STATEMENT (of this Report) Approved for public release; distribution unlimited.			
17. DISTRIBUTION STATEMENT (of the abstract entered in Block 20, if different from Report)			
18. SUPPLEMENTARY NOTES			
19. KEY WORDS (Continue on reverse side if necessary and identify by block number) Cage Instabilities Ball Bearings Gyro Bearings			
20. ABSTRACT (Continue on reverse side if necessary and identify by block number) Analytical simulations of the dynamic performance of a DMA ball bearing are obtained under a range of operating conditions. The predicted torques with Coulomb type friction characteristics seem to be within the range of the experimentally observed torque values. Also there is a general agreement between the observed torque dependence on speed and the trends predicted by the analytical simulations. A systematic parametric study over the various possible traction models covering both elastohydrodynamic and boundary friction			

DD FORM 1 JAN 73 1473 EDITION OF 1 NOV 65 IS OBSOLETE

SECURITY CLASSIFICATION OF THIS PAGE (When Data Entered)

78 07 13 027

224 550

JLC

SECURITY CLASSIFICATION OF THIS PAGE(When Data Entered)

regimes suggests that the test DMA bearing works more in the boundary friction domain or perhaps a mixed regime.

SECURITY CLASSIFICATION OF THIS PAGE(When Data Entered)

FOREWORD

Development of a fairly sophisticated Dynamics of Rolling Element Bearings (DREB) computer program was completed at MTI in July 1977. This program was sponsored by several commercial companies around the world. This project, which has been aimed at predicting the torque in Despun Mechanical Assembly (DMA) bearings, constitutes one of the first practical applications of an advanced computer program such as DREB. A number of computerized simulations of the dynamic bearing performance have been obtained and the bearing torques have been compared with the experimental observations.

ACCESSION for		
NTIS	White Section	<input checked="" type="checkbox"/>
DDC	Buff Section	<input type="checkbox"/>
UNANNOUNCED		<input type="checkbox"/>
JUSTIFICATION.....		
BY.....		
DISTRIBUTION/AVAILABILITY CODES		
Dist.	AVAIL. and/or	SPECIAL
A		

TABLE OF CONTENTS

<u>Section</u>		<u>Page</u>
I.	INTRODUCTION.	1
II.	GENERAL CHARACTERISTICS OF A DMA BEARING.	3
III.	EXPERIMENTAL TORQUE DATA.	9
IV.	ANALYTICAL SIMULATIONS.	17
V.	CONCLUSIONS	37
VI.	RECOMMENDATIONS FOR FUTURE RESEARCH	38
VII.	REFERENCES.	40

LIST OF ILLUSTRATIONS

<u>Figure</u>		<u>Page</u>
1.	Experimental Torque at 89 N Thrust Load [9].	10
2.	Experimental Torque Data at 178 N Thrust Load [9].	11
3.	Experimental Torque Data with 267 N Thrust Load [9].	12
4.	RMS Variation in Torque Under 89 N Thrust Load [9].	13
5.	RMS Variation in Torque Under 178 N Thrust Load [9].	14
6.	RMS Variation in Torque Under 267 N Thrust Load [9].	15
7.	The Nature of a Typical Elastohydrodynamic Traction Curve. . .	18
8.	Schematic Description of the Possible Traction Parameters expected to be applicable to DMA bearings.	20
9.	Dimensionless Torques per Ball for Traction Model I at 267 N Thrust Load and 60 rpm	21
10.	Race Torque per Ball at 267 N Thrust Load and Varying Outer Race Speeds.	23
11.	Race Torque per Ball Variations at a Light Load of 89N and varying speeds.	24
12.	Variations in Race Torques as a Function of Outer Race Speed.	25
13.	Typical Ball Mass Center Accelerations at 89 N and 10 rpm. . .	26
14.	Typical Variations in Ball Mass Center Positions at 89N and 10 rpm.	27
15.	Typical Angular Acceleration of the Ball at 89 N and 10 rpm. .	28
16.	Variations in Ball Angular Velocity at 89 N and 10 rpm Outer Race Speed.	29
17.	Contact Angle, Load, and Ball/Race Spin-to-Roll Ratios at 89 N and 10 rpm	30
18.	Variations in Torque with Constant Friction Coefficient at 267 N and 60 rpm.	32
19.	General Characteristics or Local Slip and Tractive Force Variations in the Ball/Race Contact Ellipse Under Constant Friction Coefficient.	33
20.	Torque Variations with a Negative Traction Slip Slope ($\kappa =$ 0.030 - 1.0 μ) at 267 N and 60 rpm.	35

SECTION I

INTRODUCTION

The coupling between the complex geometrical parameters and rather sophisticated operating conditions introduces great difficulties in the development of a realistic analytical model for rolling bearing performance simulation. In applications concerning bearing torque variations, cage instabilities, skidding and failures associated with other dynamic factors strongly need an analytical model which treats the various geometrical interaction and the lubrication mechanics fairly well. Primarily due to the extreme complexities associated with such a model, progress in this technological area has been slow.

Most of the rolling bearing models have been restricted to quasi-static type of analyses [1-3]* where a static force balance is performed on the bearing elements. Such a model has generally been good for computing the overall load distributions and the resulting fatigue life of the bearing. However, for simulating torque variations, cage instabilities, and similar dynamic parameters, it is necessary that the classical differential equations of motion be formulated and integrated in time to obtain a real-time simulation of bearing performance. Walters [4] presented a dynamic model for a ball bearing which considered the cage with complete generality but constrained the ball motion such that the ball mass centers are forced to move along a path predetermined by quasi-static type of models [1-2]. Thus such a model is free of any ball-race vibrations, dynamic changes in race loads and speeds, and similar transient factors which sometimes play a dominant role in establishing the torque variations in the bearing and perhaps the instabilities of the cage motion. Gupta [5] treated an angular contact ball bearing with a pure thrust load. In this work the ball motion was considered with complete generality, but the bearing was considered to be cageless. Very recently, Gupta [6] has developed a generalized dynamic model where all the rolling elements, the cage, and both races are treated with all the generalities of the classical differential equations of motion in the full six-degrees-of-freedom system. Also, this model considers both ball and roller bearings, and it provides a great flexibility in terms of operational variables such as load and speed variations, lubricant models, etc.

*Numbers in brackets denote references.

The model is presented in terms of a Dynamics of Rolling Element Bearings (DREB) computer program. Such a computerized simulation for the first time provides a means to estimate torque variations in a rolling bearing under prescribed operating conditions.

Since bearing torque plays a dominant role in Despun Mechanical Assembly (DMA) systems, a realistic model which predicts the bearing torque and torque variations is necessary. Although such an application is free of any high-speed effects, since the general operational speeds are quite low, the lubrication mechanics and the resulting ball-race friction introduce great difficulties in the torque computations. The objective of the present program is to evaluate the torque predictions, as given by the computer program DREB, in the light of some available experimental data. Such a validation will strengthen the capabilities of DREB to predict torque in DMA bearings. Hence, the needed analytical model for the bearing performance simulation can be derived and the procedures for the DMA bearing design and failure diagnosis can be greatly improved.

Although a number of experimental questions remain unanswered and a realistic traction model for the DMA bearing application has yet to be determined, it is shown that DREB provides a fairly realistic simulation of bearing torque variations. Also, the predicted values are in the neighborhood of the experimental observations under certain traction parameters. The next section of this report deals with the bearing details and some general operational characteristics. The available experimental torque data and the experimental limitation are then discussed in Section III. Finally, a number of analytical simulations are obtained with the use of the computer program DREB and the analytical simulations are compared with the experimental data.

SECTION II
GENERAL CHARACTERISTICS OF A DMA BEARING

A typical DMA application employs a 100-mm bore angular contact ball bearing. The bearing operates at a relatively low speed, and it is mostly thrust loaded. Although a cage is used in many applications, the question of removing the cage and eliminating cage instabilities is still unanswered. It is this question which has led to experimental test programs with full complement or cageless bearings. The present investigation also emphasizes cageless bearing, and it is assumed that under pure thrust load no significant ball-to-ball collisions take place. Some of the bearing and operational details are discussed below.

Bearing Geometry

The geometrical details of the cageless bearing are as follows:

Bore	= 0.100	M
Outside Diameter	= 0.150	M
Ball Diameter	= 0.015875	M
Pitch Diameter	= 0.1250	M
Contact Angle	= 26.0	degrees
Number of Balls	= 24	
Outer Race Curvature Factor	= 0.52	
Inner Race Curvature Factor	= 0.52	

The same bearing has been used with the cage when the number of balls is reduced to 19. Since the present investigation emphasizes a cageless bearing, the details of cage geometry are omitted.

Materials

Both races and all the balls are assumed to be made of conventional ball bearing steel with the following relevant properties:

Elastic Modulus	= 2.0×10^{11} N/M ²
Poisson's Ratio	= 0.25
Mass Density	= 7.75×10^3 kgm/M ³

The above properties are practically unchanged for a wide range of bearing steels with varying compositions and hardnesses.

Lubricant

Most of the experimental data, described in the next section, was obtained with a typical space application lubricant which has been described as "Lubricant A" by Rivera [7] and as "Apiezon C + 1.5 percent Antioxidant" by Tyler, et al. [8]. There is no traction data available on this lubricant. However, the general viscosity characteristics have been described by Tyler, et al. [8] as follows:

Kinematic Viscosity ν ($M^2/s \times 10^6$) is given by:

$$\log \log (\nu + 0.60) = A - B \log (T + 273) \quad (1)$$

where T is the temperature in $^{\circ}C$ and A and B are constants having values of 9.41058 and 3.65489, respectively.

The pressure viscosity coefficient, α , in the relation $\mu = \mu_0 \exp (\alpha p)$ is given by:

$$\alpha = \frac{K}{T} \quad M^2/N \quad (2)$$

where T is temperature in $^{\circ}C$ and K and C are once again constants having values of 12.13×10^8 and 0.471, respectively.

The specific gravity γ at any temperature T ($^{\circ}C$) is expressed as:

$$\gamma = \gamma_{15.6} - G(T - 15.6) \quad (3)$$

where $\gamma_{15.6}$ is the specific gravity at 15.6 $^{\circ}C$ and it is equal to 0.879 and G is a constant having a value of 0.00070.

The temperature viscosity coefficient for the relation $\mu = \mu_0 \exp \{\beta (1/T_0 - 1/T)\}$ is estimated from Equation (1) to be approximately 6000 $^{\circ}K$ in the neighborhood of the operating temperature discussed in the following paragraphs.

No data is available for the thermal conductivity of the lubricant; however, it is assumed to be 0.10 N/S/°C as it is for most lubricants.

Operating Conditions

The thrust load on the bearing varied from 89 to 267 N while the outer race speed ranged from 5 to 60 rpm. The inner race is held fixed, and it carries the torque measuring devices. Although there is a certain uncertainty about the operating temperature, it is assumed to be 15°C [9]. Some of the lubricant properties at this temperature, in accordance with the relations described in the preceding paragraph, will be:

Viscosity, μ	= 0.382 NS/M ²
Pressure Viscosity Coefficient, α	= 3.39×10^{-8} M ² /N
Temperature Viscosity Coefficient, β	= 6000 °K
Thermal Conductivity	= 0.10 N/S/°C
Mass Density	= 8.745×10^2 kgm/M ³

For the above properties, computations were made to determine the elastohydrodynamic (EHD) film thickness and possible lubricant drag on the ball. The results will be discussed below.

Elastohydrodynamic Film Thickness

The computer program DREB is used to compute the EHD film thickness over the range of loads and speeds. The results are described in Table I.

All the results presented in Table I are under fully flooded conditions. In the case of DMA bearings, where the lubricant quantity is highly limited, the actual film thickness may be very much smaller than these values.

In order to establish the type of contact, the film thickness values must be compared with the surface roughness values. Although the actual surface roughness data is not available, it is expected that the ball has a surface finish of about 2.5 to 5.0×10^{-8} M and that on the race is about 1.0 to 3.0×10^{-7} M [9]. It may, therefore, be concluded that EHD conditions will exist only with the

TABLE I
ELASTOHYDRODYNAMIC FILM THICKNESS COMPUTATIONS

Bearing Thrust Load (N)	Outer Race Speed (RPM)	Film Thickness (M)	
		Outer Race Contact	Inner Race Contact
267	10	1.18×10^{-7}	1.06×10^{-7}
267	30	2.47×10^{-7}	2.22×10^{-7}
267	60	3.88×10^{-7}	3.50×10^{-7}
89	10	1.27×10^{-7}	1.14×10^{-7}
89	30	2.61×10^{-7}	2.35×10^{-7}
89	60	4.10×10^{-7}	3.70×10^{-7}

smoothest surfaces operating under the lightest load and highest speed conditions. Also, the quantity of lubricant must be adequate to ensure fully flooded conditions. If all of these conditions cannot be met in a real bearing, then the contact will be of a boundary type friction and the EHD action will be small.

For the EHD regime of operation, it is necessary to test the lubricant for its traction characteristics while the boundary friction coefficients must be measured in case of metal contact. Unfortunately, none of these data are presently available. The objective of the present investigation is, therefore, to examine the behavior of the bearing over a range of traction parameters and evaluate the predicted torque in light of available torque data.

Lubricant Drag

When the quantity of lubricant is very limited, normally the drag forces can be neglected. However, since the measured torques are also very small in magnitude, a question was raised [9] concerning ball drag. The computer program DREB uses a simple boundary layer type of formulation [10] for computing drag on the balls. The primary input to such a computation is the effective density of the mixture of air and oil in the bearing. Generally, such an effective density is arrived at by volume averages. A rough computation indicates that a conservative estimate of the total bearing cavity is about $5.73 \times 10^{-5} \text{ M}^3$ while the volume of oil at a supply of 4 mg/ball (in range of experimental data presented in the next section) is about $1.10 \times 10^{-7} \text{ M}^3$. Thus, the volume ratio is 0.0019 which leads to an effective density of 1.67 kgm/M^3 .

The relation for drag is of the form:

$$D = C_D \rho V^2 A$$

where D is the drag force; ρ is the effective mass density; V is the ball mass center velocity; A is the frontal area; and C_D is the drag coefficient for spherical bodies [10].

It is shown [10] that at very low speeds the drag coefficient may be written as:

$$C_D = \frac{24}{R}$$

where R is the Reynolds number, $R = Vd/\nu$, d and ν being the ball diameter and kinematic viscosity, respectively.

It is seen that the drag force will be proportional to the ball velocity, which is practically independent of the bearing load and it is proportional to the race speed. The computed drag for the three race speeds is tabulated in Table II.

It is true that these drag forces are small in magnitude. However, at high-speed they could contribute to about 0.0133×0.0625 (pitch radius)/2 = 0.00042 NM of torque per ball. Thus, for a bearing with 24 balls, the total torque will be about 0.01 NM, which may be significant when compared with some of the measured torque data presented in the next section.

TABLE II
BALL DRAG FORCES

Race Speed RPM	Drag Force N
10	0.0021
30	0.0065
60	0.0133

SECTION III

EXPERIMENTAL TORQUE DATA

The experimental data used in the present investigation was obtained at the Air Force Materials Laboratory at Wright Patterson Air Force Base. The details of the experimental set-up are presented by Rivera [7], and they are omitted here for brevity.

For the bearing described in the preceding section, the measured torque as a function of lubricant quantity is presented in Figures 1 to 3*. There are three general patterns in these experimental observations. First, the torque increases with lubricant quantities and it stabilizes at some steady value, at least at the lower speeds. Secondly, the torque increases monotonically with speed. Finally, it appears that the torque has a rather low dependence on bearing load. These observations, at first sight, lead to some drag phenomenon as a principal contributor to torque. However, as will be discussed in the next section, the local slip velocities in the ball/race contact zone and the resulting tractive forces will couple with any applied drag forces and, hence, the problem becomes somewhat complicated.

The variations in torque, corresponding to the data shown in Figures 1 through 3 are shown in Figures 4 through 6. Again, it is seen that torque variations increase with speed. If any load dependence is derived from this data, it is found that the torque variations somewhat increase with the load, which is opposite of what one would normally expect. In any event, the amount of data is not adequate to derive any general conclusions about either the torque variations or the average torque values.

A number of experimental difficulties encountered during the measurement of the data presented herein must also be noted [9]. Any test rig behavior leading to slipping of the generally stationary race will contribute to torque variations. It was pointed out [9] that possibilities of such slippage do exist in the present test set-up, and a number of modifications are necessary in order to rectify the problem. Also, in view of such a problem, it is agreed that substantial confidence cannot be imposed on the measured torque variation data.

*The data was supplied to MTI by Rivera [9] of the Air Force Materials Laboratories at Wright Patterson Air Force Base.

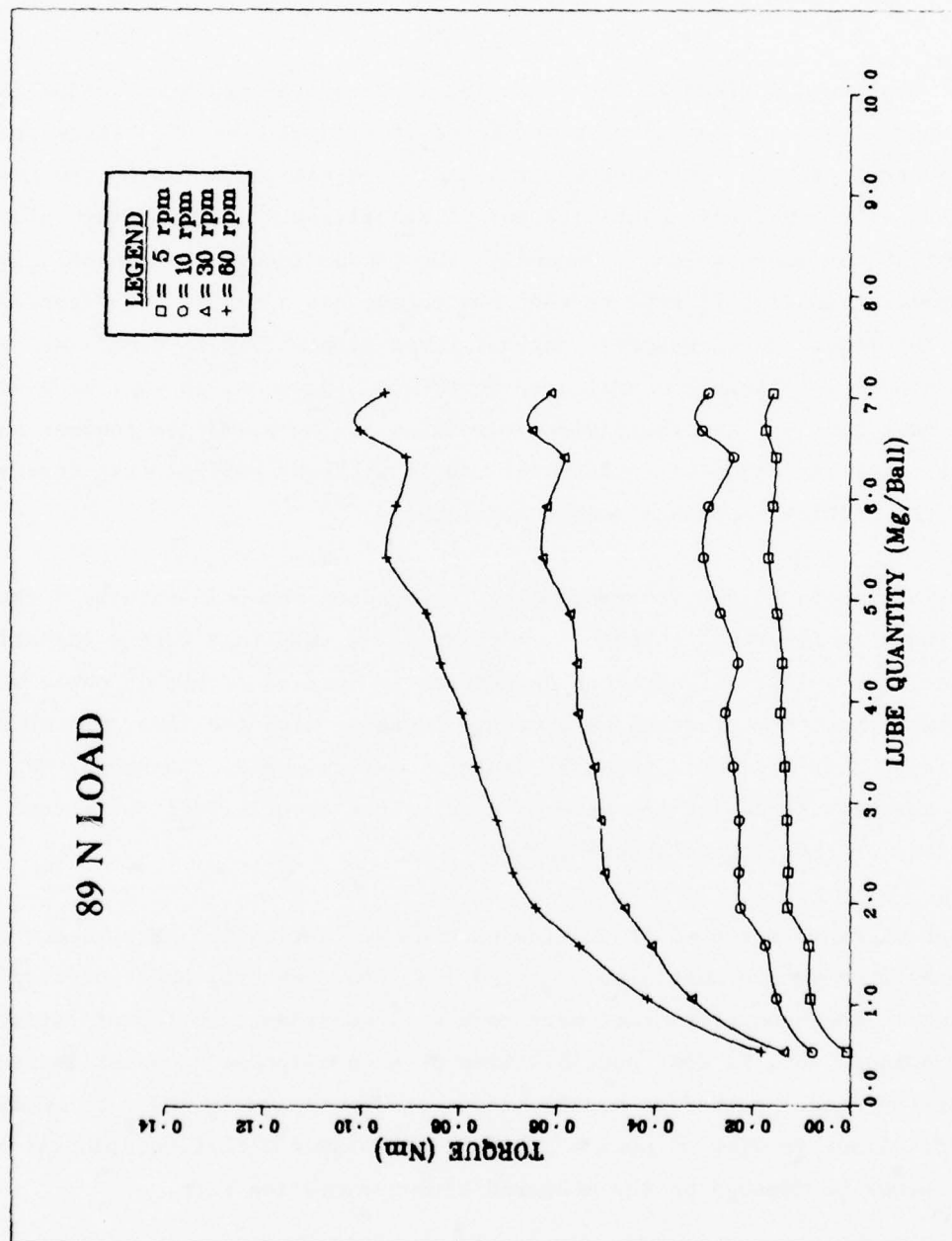


Figure 1. Experimental Torque Data at 89 N Thrust Load [9]

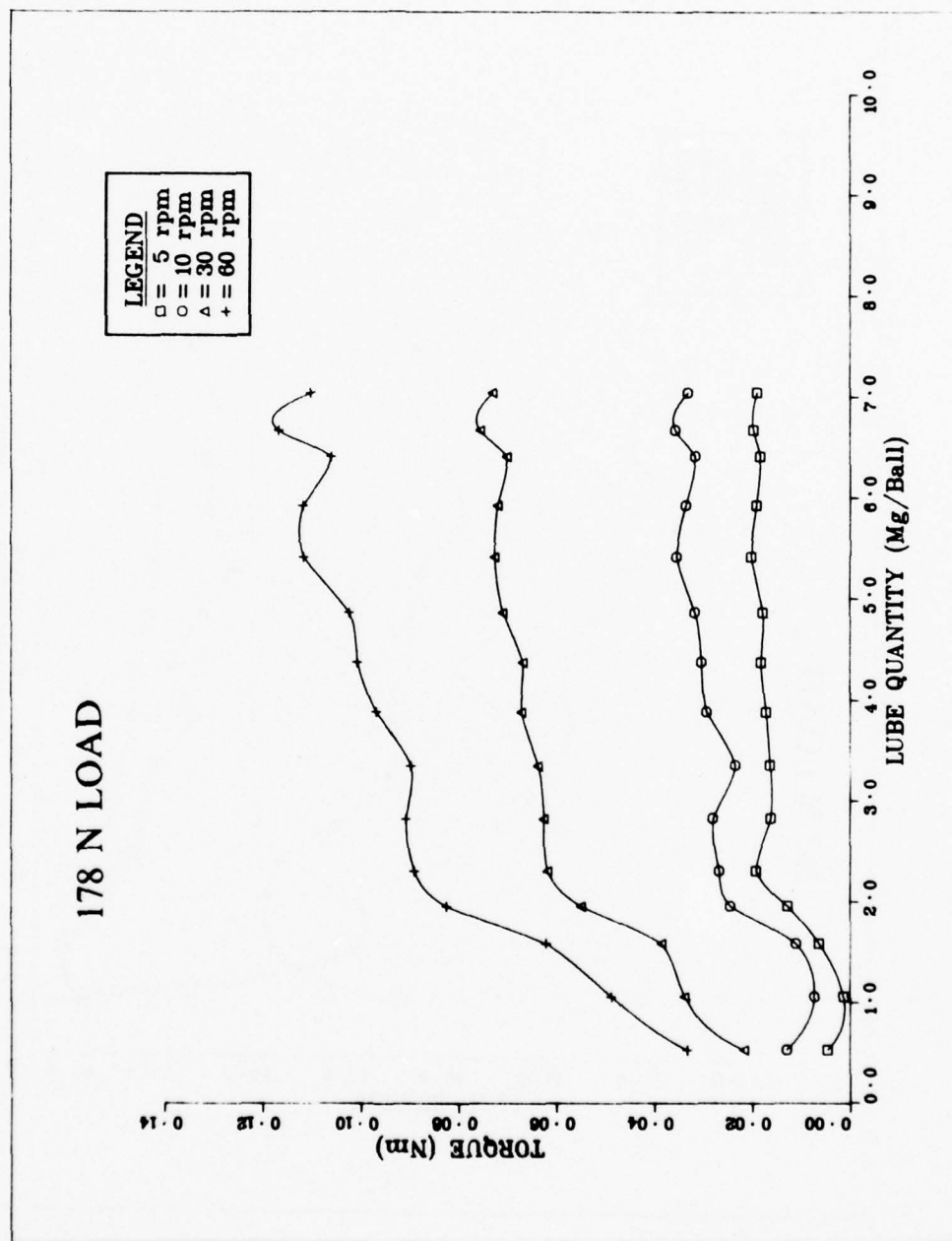


Figure 2. Experimental Torque Data at 178 N Thrust Load [9]

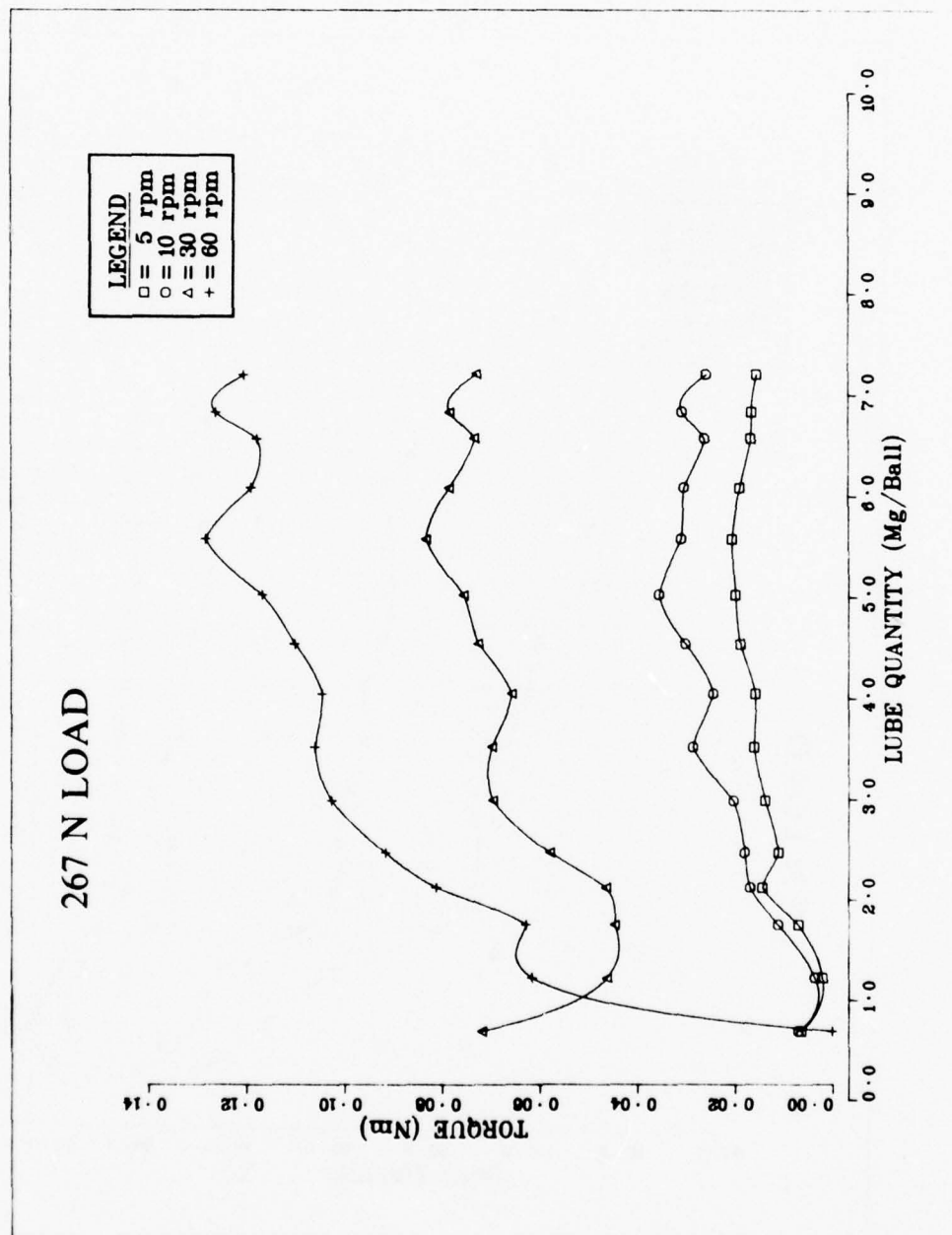


Figure 3. Experimental Torque Data with 267 N Thrust Load [9]

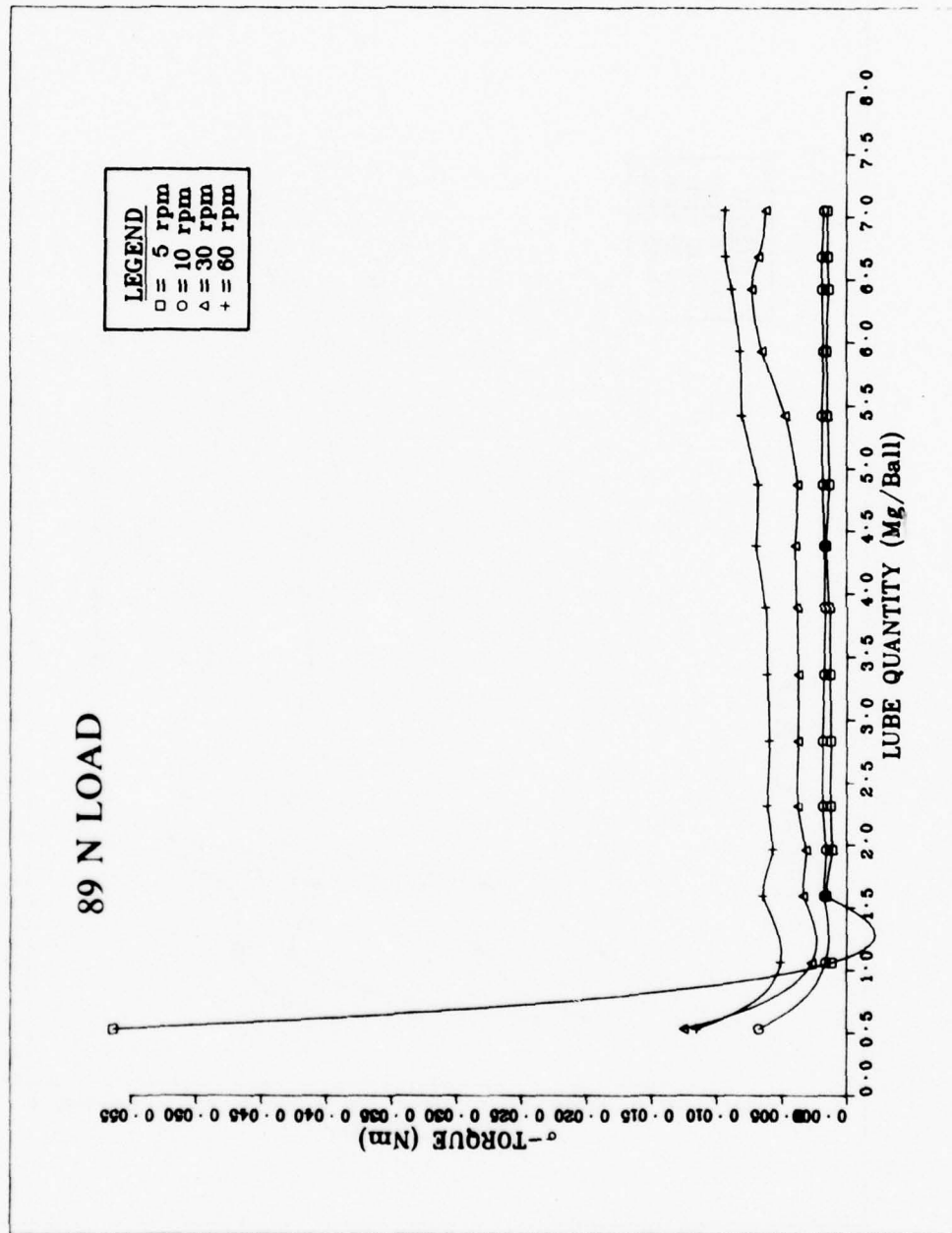


Figure 4. RMS Variation in Torque Under 89 N Thrust Load [9]

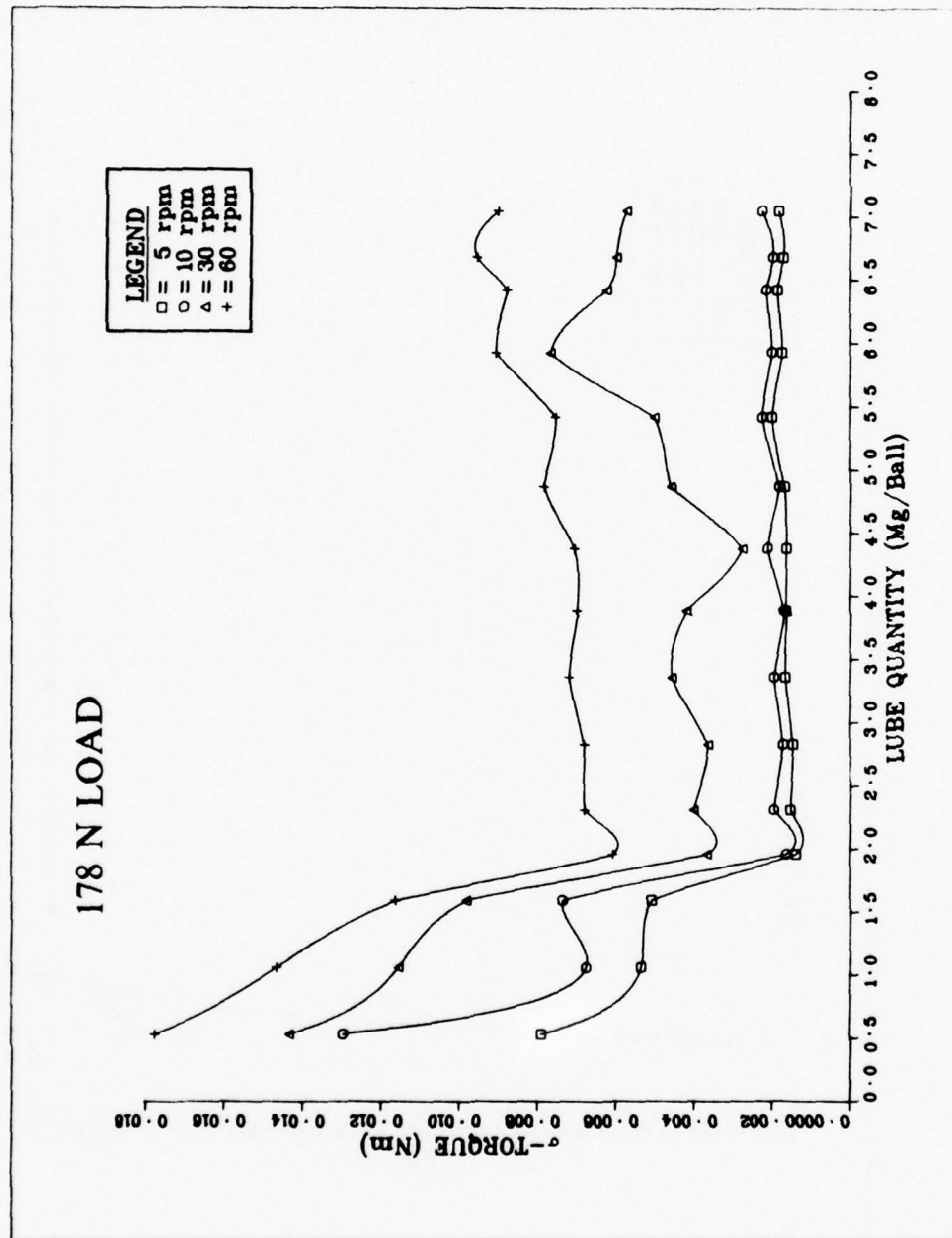


Figure 5. RMS Variation in Torque Under 178 N Thrust Load [9]

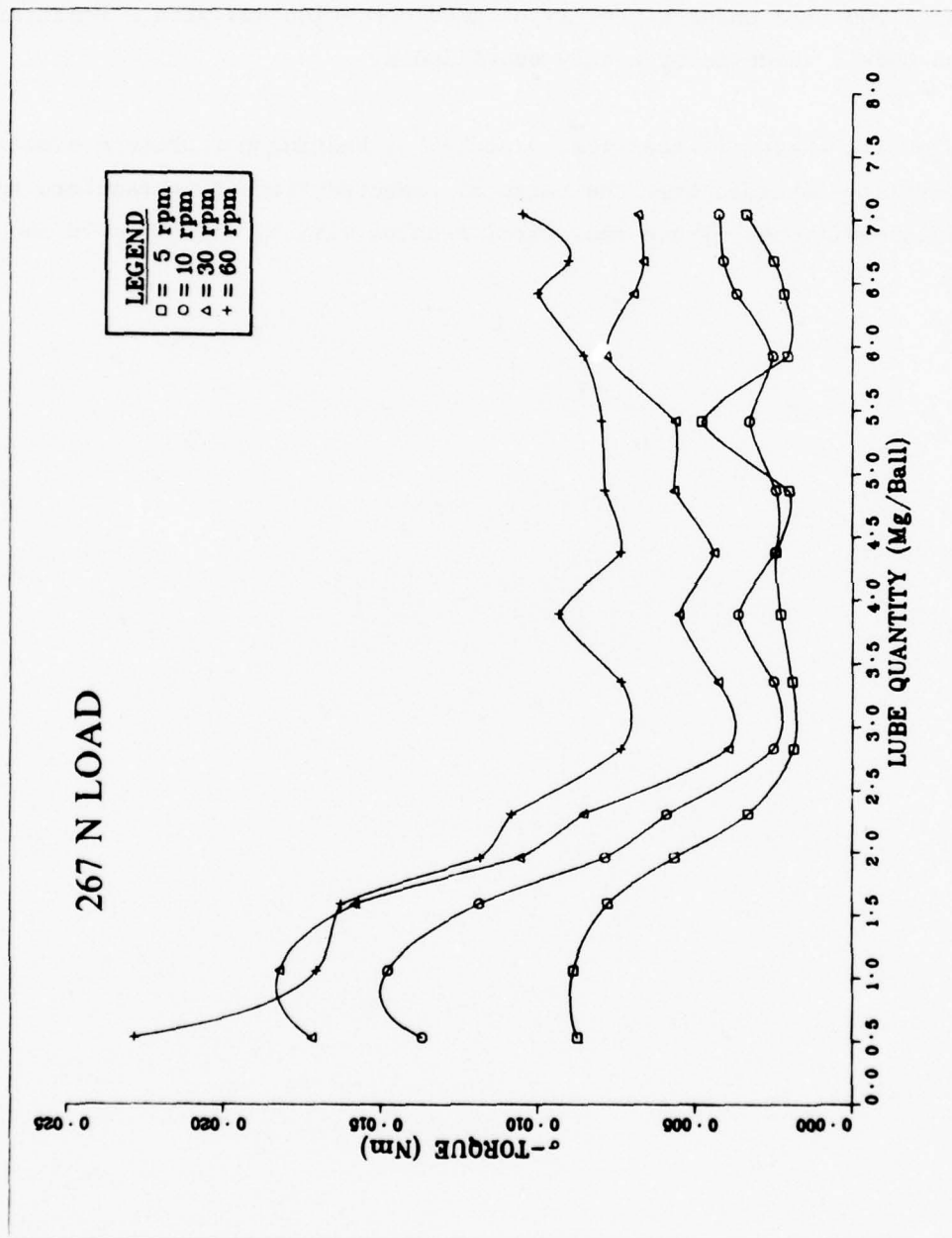


Figure 6. RMS Variation in Torque Under 267 N Thrust Load [9]

Possibilities of relative misalignment between the two races also exist in the present set-up [9]. A misalignment will generally result in increased torques due to increased irregularities in load and slip distributions over the balls. It is, therefore, expected that the measured torques may be somewhat higher than these computed under perfectly aligned condition and with a realistic traction model, which is presently unavailable.

In view of all these difficulties, a number of bearing performance simulations using DREB are obtained over the range of expected traction parameters and operating conditions. These analytical results will be discussed in the next section.

SECTION IV

ANALYTICAL SIMULATIONS

For a purely thrust loaded cageless bearing, such as the DMA ball bearing, a considerable computer time can be saved by proper modelling of the bearing such that the motion of only one ball is examined. Such a model will be reasonable since all the balls behave identically in a purely thrust load bearing. The details of the model will be discussed below.

Traction model is another significant input to the bearing performance simulation. Since no traction model is available for the lubricant under consideration, it is necessary to cover a range of traction parameters, which possibly include both the EHD and the boundary friction regimes. Some details of the traction models used will also be discussed below before presenting the various simulations.

The Bearing Model

In a low-speed, lightly load angular contact thrust ball bearing, the nominal load distribution on all the balls is uniform and it can be very readily determined by conventional quasi-static analysis. For the DMA bearing, it is, therefore, necessary to do such a computation and determine the relative position of the races for the prescribed loads and speeds. The race mass centers may now be constrained to stay fixed in these relative positions as the dynamics of a ball is closely examined. Also, since all balls behave identically, it is only necessary to examine one ball.

The above assumptions and the use of DREB are a considerable improvement over an earlier thrust bearing model [5] which forces the inner race to be in static equilibrium, i.e., the inner race is assumed to be massless. In the DMA bearing testing the assumption of holding the races fixed in space is much more realistic [7,9] and hence such a constraint is used in DREB for all the simulations.

Traction Model

Figure 7 shows the nature of a typical traction slip relation under elastohydrodynamic conditions. The traction increases to a maximum value and, with continually increasing slip, it reduces to an asymptotic value. For applications with very low slip rates, such as the DMA Bearing, the critical parameter will be the slope of the traction curve near zero slip. Hence, in the absence of a traction model, it will be essential to cover a wide range of slopes.

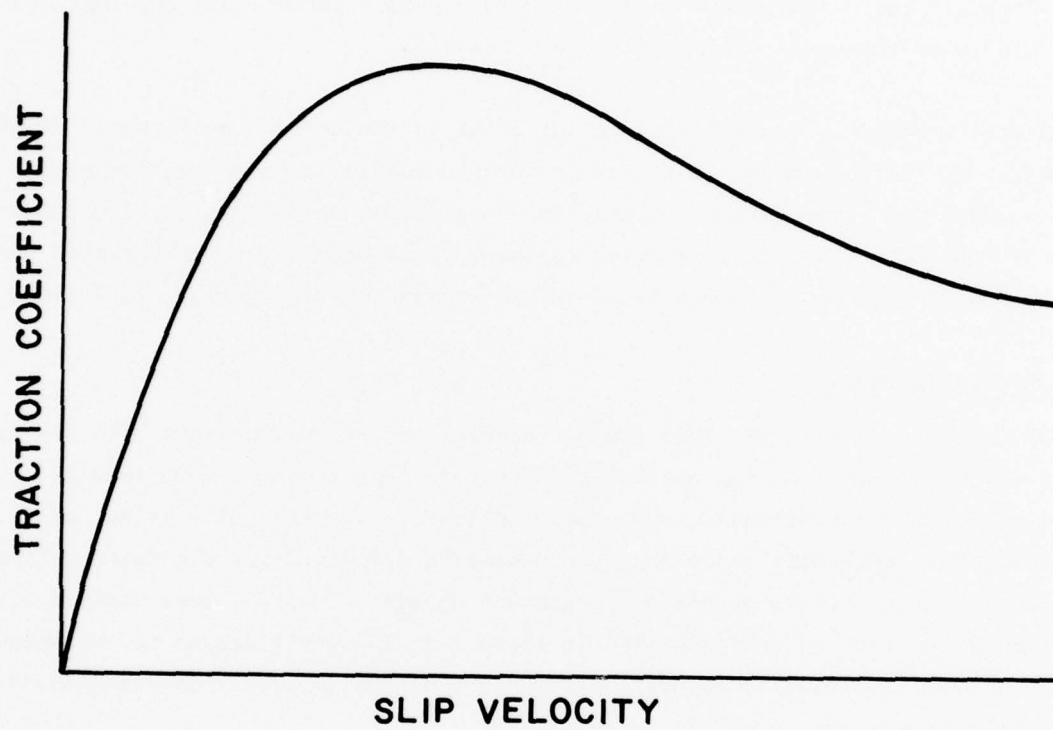


Figure 7. The Nature of a Typical Elastohydrodynamic Traction Curve

In the case of boundary friction, the traction coefficient may become independent of slip and the model may just reduce to a constant friction coefficient. In some cases of dry friction it is found that the friction coefficient reduces with increased slip [11] and terms such as "static" and "kinetic" friction coefficient have been introduced.

In view of all the above possibilities, three models are considered in the present investigation. The models are schematically described in Figure 8. The Model I basically represents the slope of a typical elastohydrodynamic traction curve shown earlier in Figure 7. Model II is a Coulomb type constant friction coefficient. Finally, Model III represents the classical static to kinetic friction transition in dry metal contacts. It is expected that all these models will cover a wide range of possibilities including the boundary friction and elastohydrodynamic regimes for the DMA bearings.

Simulation for Model I - ($\kappa = Bu$)

For a prescribed bearing load and speed, three values of the slope, B , are selected to cover a wide range and the bearing performance is simulated. The dimensionless torques for the varying slopes are shown in Figure 9. It is seen that the bearing torque reaches a steady value, which is practically independent of the slope B . However, the time required to reach a steady value is dependent on the slope, as might be expected. The frequent ripples in the case with $B = 10$ perhaps result from very large changes in traction due to slight changes in slip rates, which may result from gyroscopic rotations or excitations of the bearing characteristic vibration frequencies (which will be discussed later), and they are highly transient in the analytical simulations. However, in practical applications, if the bearing is continually subjected to small vibrations from the other parts of the system, such ripples could be steady state and the amplitude will be dependent on the nature of the disturbance imposed.

The magnitudes of the torques shown in Figure 9 are quite small. In fact, when the values are converted to dimensional numbers, they are about 4.7×10^{-4} and 3.6×10^{-4} NM/Ball, respectively, for the outer and inner races. For 24 balls, the total torques about the bearing axis will be 0.011 and 0.0086 NM, respectively, on the outer and inner races. From the magnitude of these values

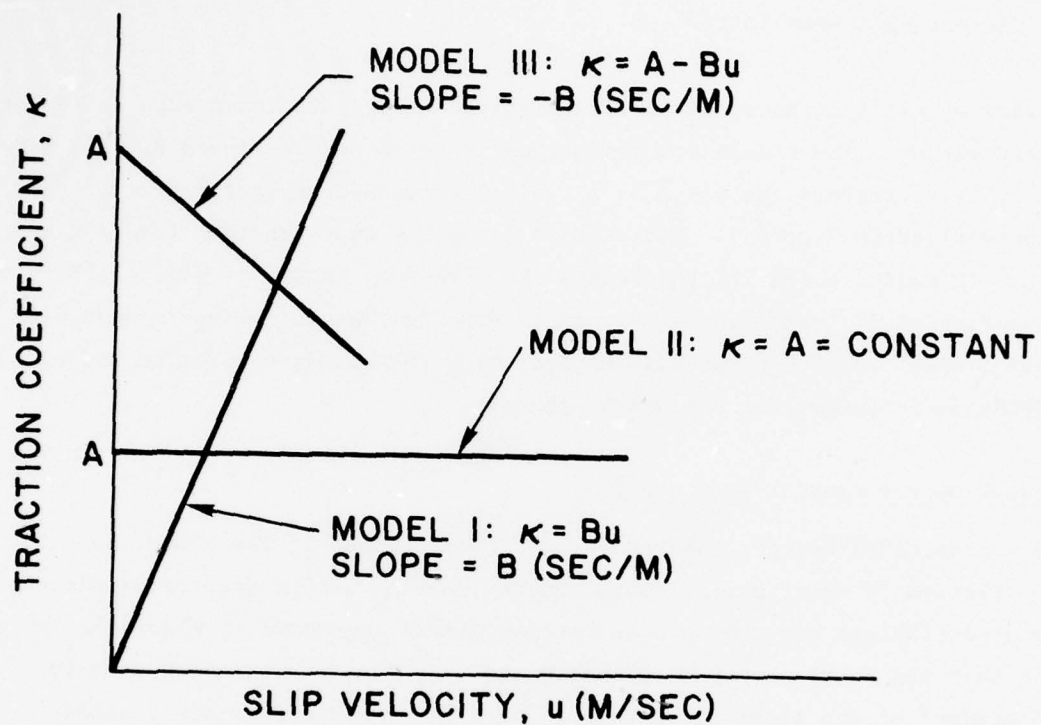


Figure 8. Schematic Description of the Possible Traction Parameters expected to be applicable to DMA bearings

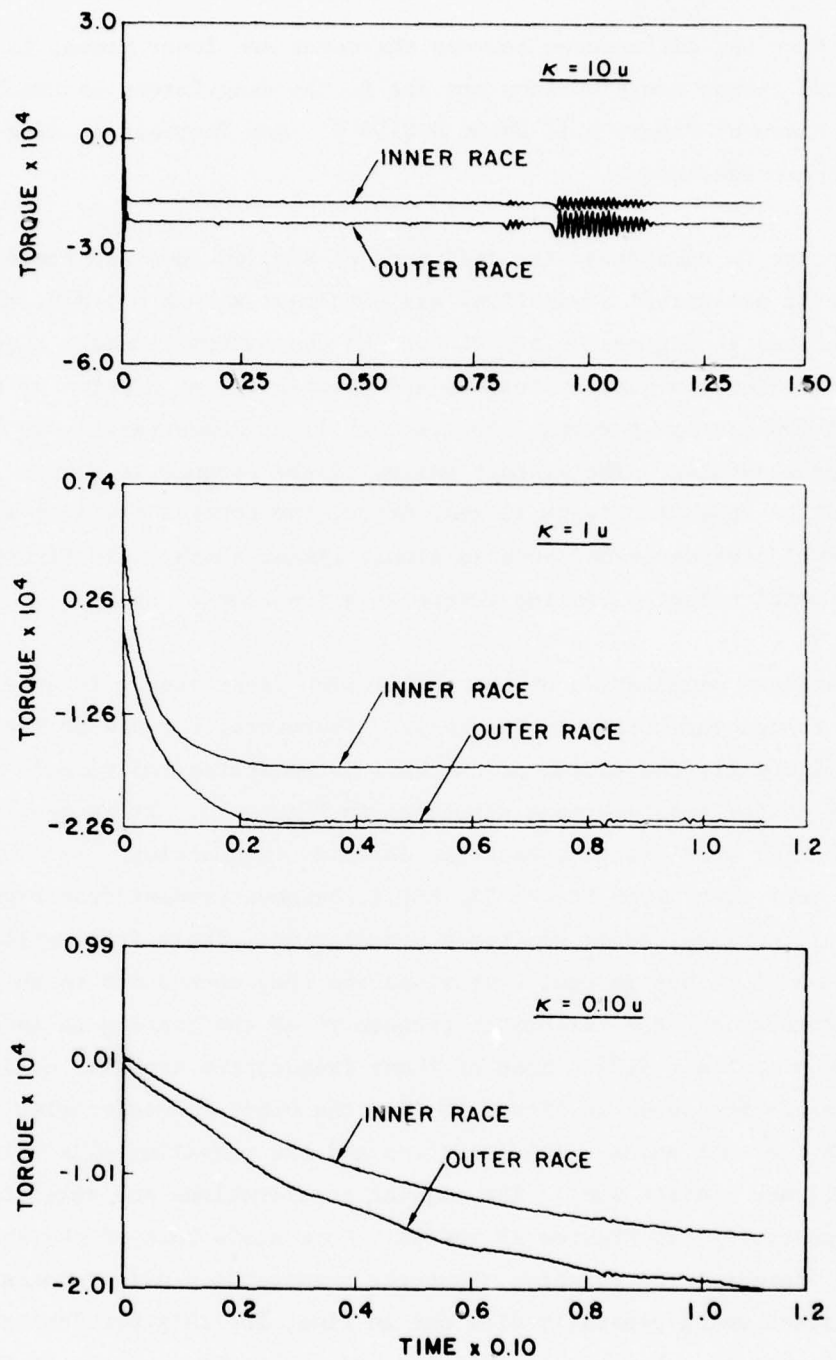


Figure 9. Dimensionless Torques per Ball for Traction Model I at 267 N Thrust Load and 60 rpm. Scales factors for torque and time are, respectively, 2.118 N and 6.949×10^{-4} seconds.

and from the differences between the outer and inner races, it seems that most of the torque contributions are due to the drag forces on the ball, which for the cases of Figure 9 is about 0.0133 N. Any increase in drag will proportionally increase the torque.

In order to understand the influence of applied load and speed on overall torque several additional simulations are obtained; with $B = 1$ S/M, these results are described in Figures 10 and 11 for the two extreme loads. Figure 10 shows fairly steady values of torques and practically no ripples of a size comparable with the average torques. However, at light loads relatively large torque ripples develop. The average values of the torques in Figure 11 are almost equal to those in Figure 10 and, hence, the torques are load-independent. The general dependence on speed is almost linear as shown in Figure 12, which shows the total computed bearing torque as a function of speed.

A detailed examination of the ball motion is necessary in order to understand the torque variations in Figure 11. Therefore, for one of the cases outlined in Figure 11, the motion of the ball is monitored and closely examined. The mass center accelerations are shown in Figure 13. It is seen that the radial and axial accelerations have two definite frequencies. The low frequency is not very clear from Figure 13, but it becomes evident from Figure 14 where the resulting mass center positions are plotted. These frequencies are about 8.1 kHz and 1.20 kHz in real dimensions and they correspond to the "elastic contact frequency" and the "kinematic frequency" of the bearing as identified earlier by Gupta, et al. [12]. Some of these frequencies are also evident in the orbital acceleration shown in Figure 13, but the orbital acceleration is also coupled with the ball angular accelerations and the resulting slip velocities in the ball/race contact zone. The angular accelerations and velocities are shown, respectively, in Figures 15 and 16. Once again both of the above frequencies are present. The rotation about the transverse y axis denotes a gyroscopic rotation which generally dies out in time, for this particular case, as seen in Figure 16. However, a definite spin velocity develops at the inner race, as shown in Figure 17 and the bearing is not "outer race controlled" as assumed in most quasi-static simulations. Figure 17 also shows the variations in contact loads and angles.

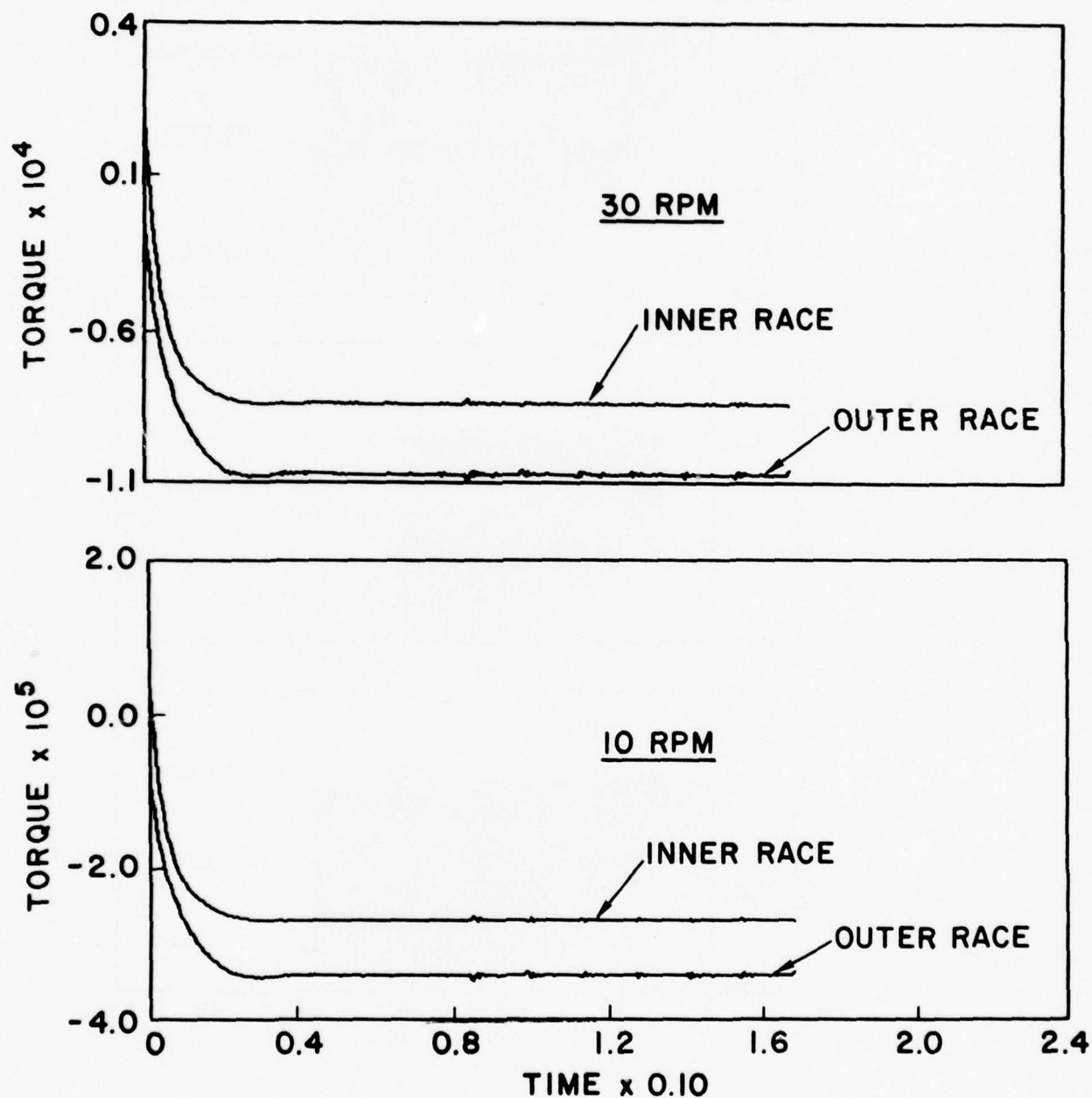


Figure 10. Race Torque per Ball at 267 N Thrust Load and Varying Outer Race Speeds. (See Figure 9 for 60 rpm.) $\kappa = 1.0$ u and the torque and time scales are 2.118 NM and 6.949×10^{-4} second.

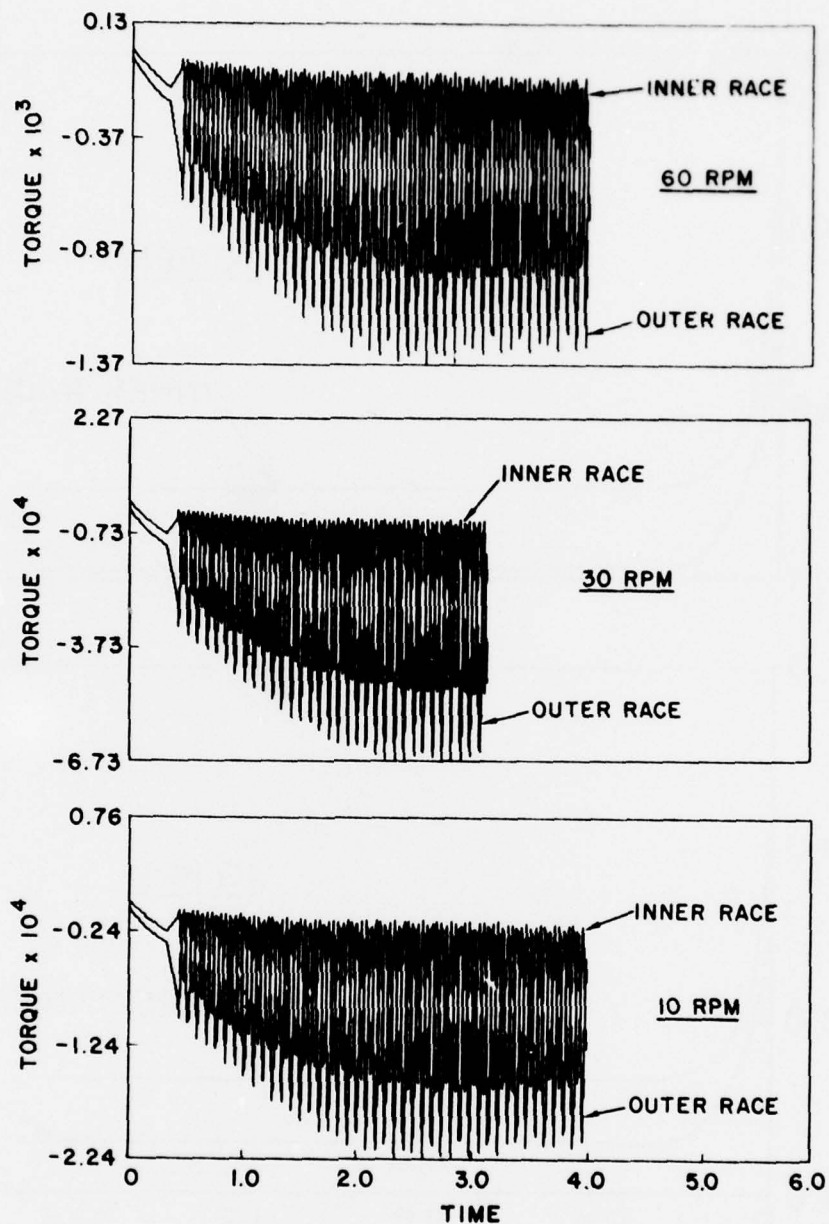


Figure 11. Race Torque per Ball Variations at a Light Load of 89 N and varying speeds. Traction model $\kappa = 1.0$ u and the torque and time scales are respectively 0.7062 NM and 1.204×10^{-3} sec.

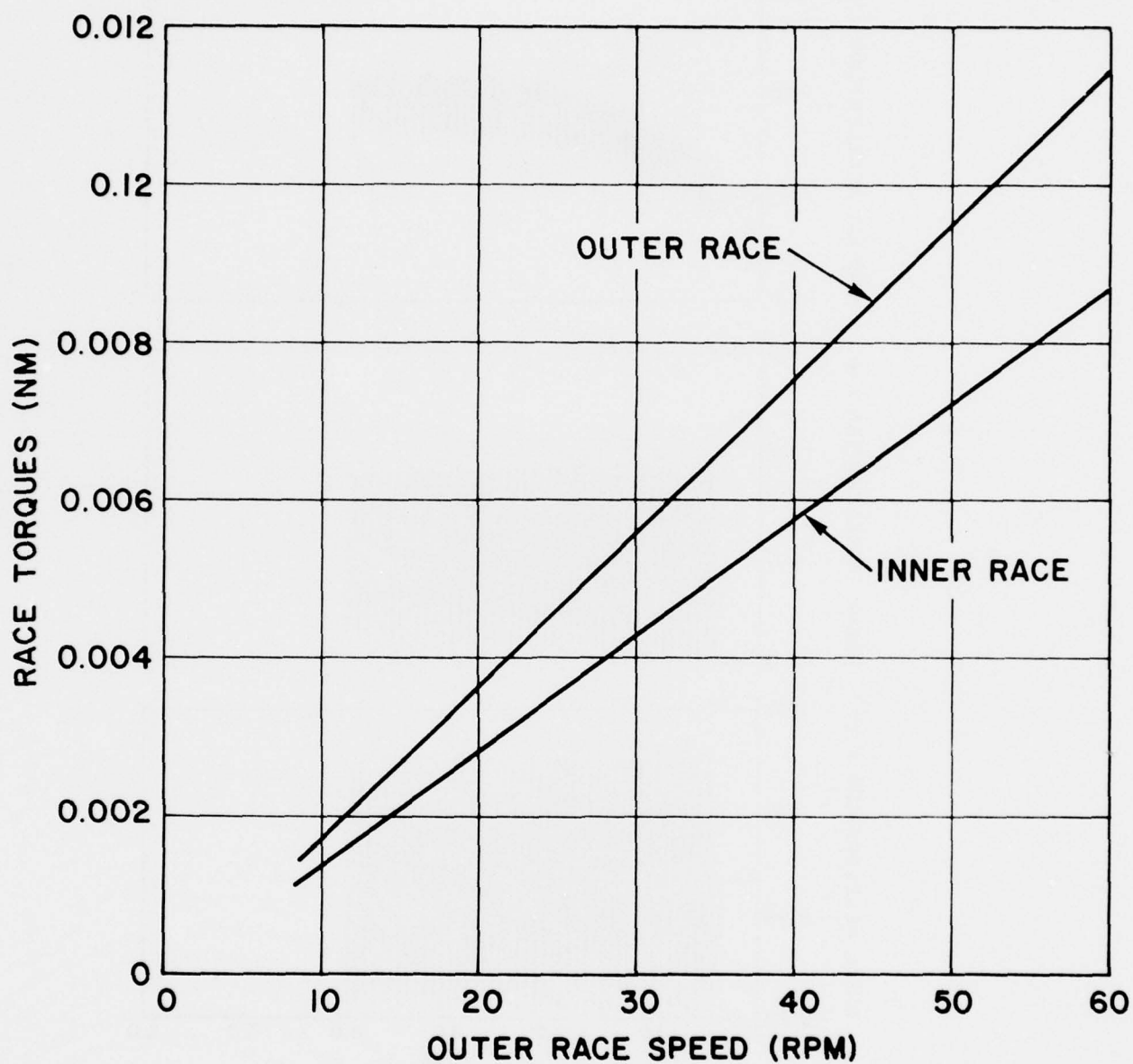


Figure 12. Variations in Race Torques as a Function of Outer Race Speed. The inner race is held stationary and the traction model is $\kappa=1.0$ u.

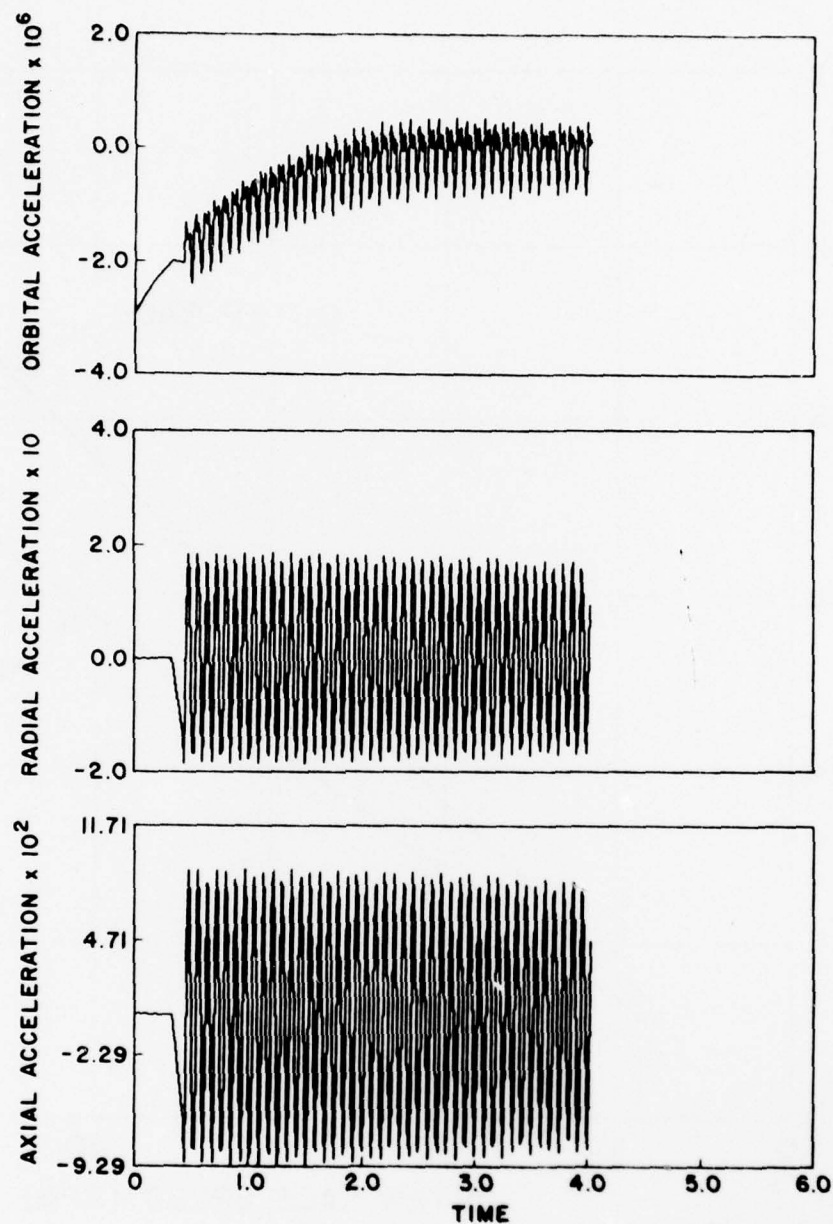


Figure 13. Typical Ball Mass Center Accelerations at 89 N and 10 rpm. The force, length and time scales are 89 N, 7.937×10^{-3} M and 1.204×10^{-3} sec. Traction model is $\kappa = 1.0$ u.

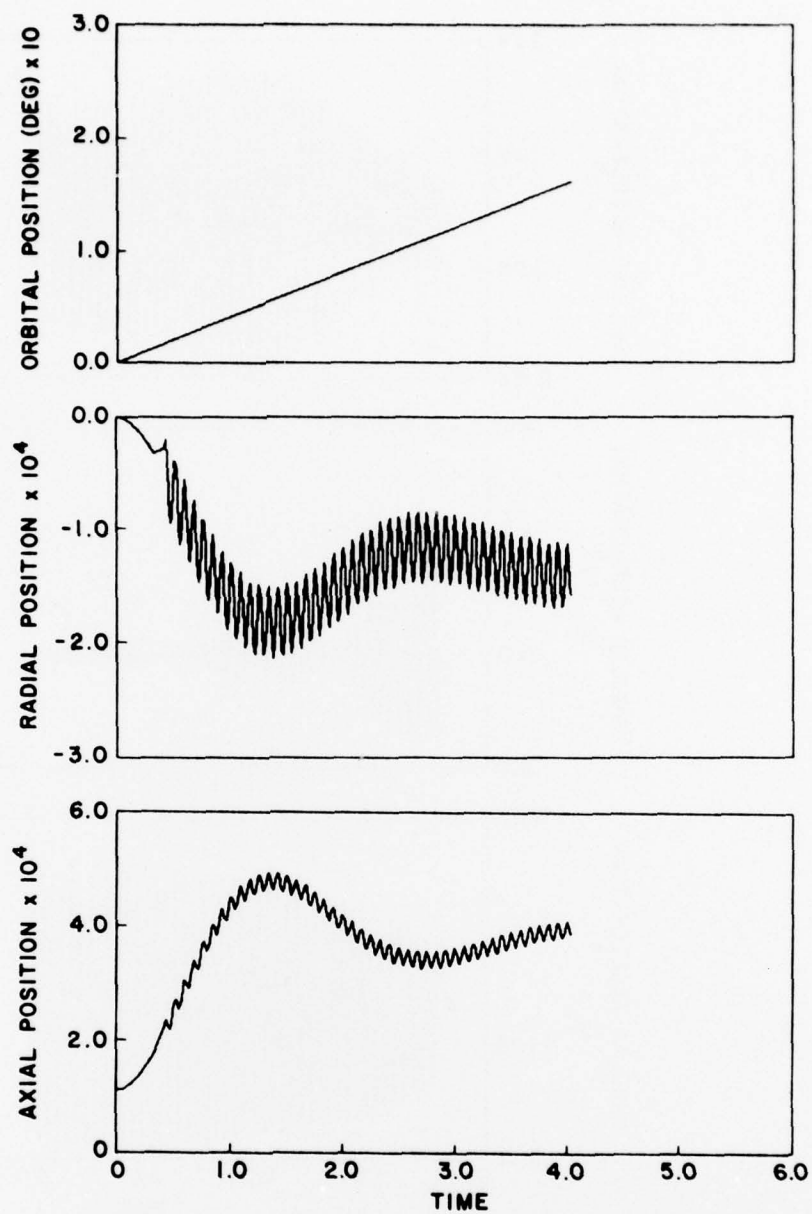


Figure 14. Typical Variations in Ball Mass Center Positions at 89 N and 10 rpm. The length and time scales are 7.937×10^{-3} M and 1.204×10^{-3} sec respectively. Traction model is $\kappa = 1.0$ u.

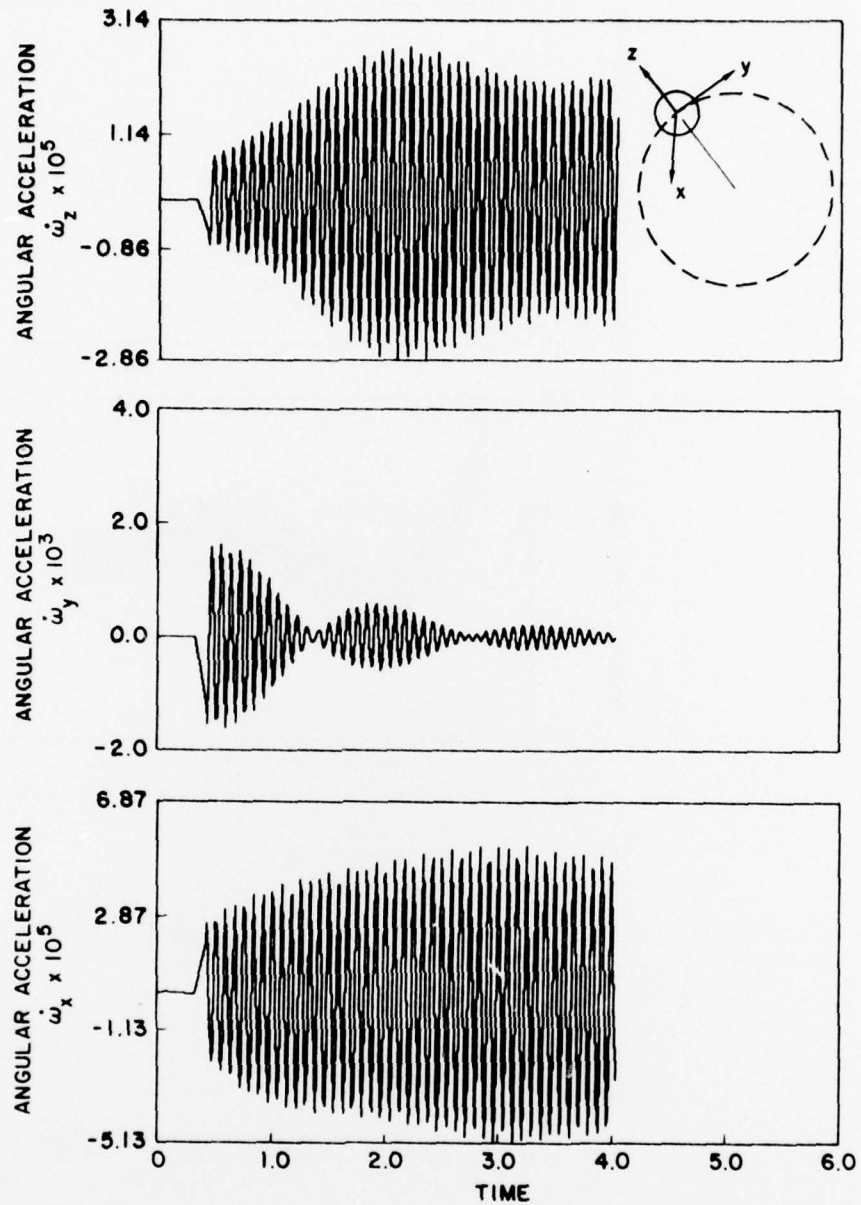


Figure 15. Typical Angular Acceleration of the Ball at 89 N and 10 rpm. The time scale is 1.204×10^{-3} sec and the traction model is $\kappa = 1.0$ u.

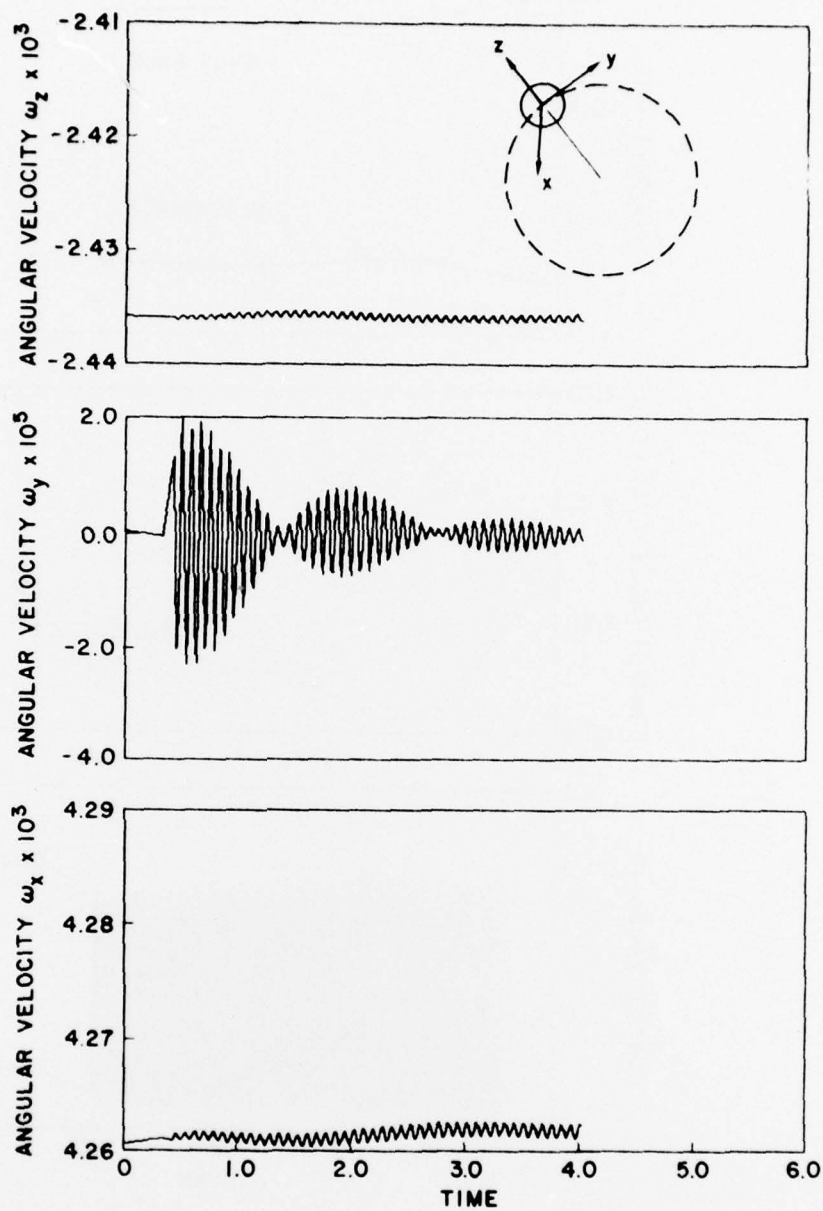


Figure 16. Variations in Ball Angular Velocity at 89 N and 10 rpm Outer Race Speed. The time scale is 1.204×10^{-3} sec and the traction model is $\kappa = 1.0$ u.

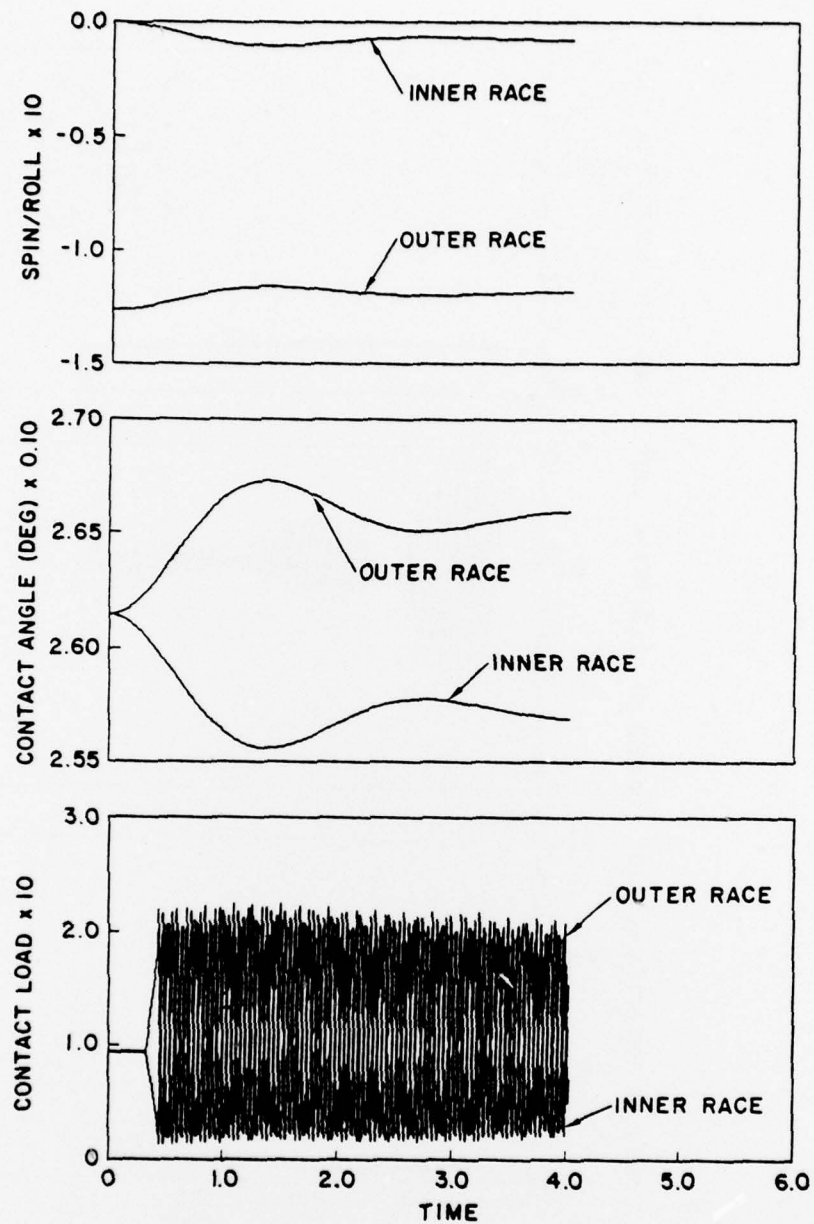


Figure 17. Contact Angle, Load, and Ball/Race Spin-to-Roll Ratios at 89 N and 10 rpm. The load and time scales are 89 N and 1.204×10^{-3} seconds, respectively, and the traction model is $\kappa = 1.0$ u.

All the above dynamic variations couple, and they result in variations in torque as seen earlier in Figure 11.

A comparison of the above torque results with the experimental data shows that, although the speed trends are in somewhat of an agreement, the general predicted values are very much lower than those observed experimentally. However, it must be remembered that a valid comparison between the predicted values and the experimental values is not possible in the absence of a true traction model. Therefore, further discussion on this subject is postponed until the later part of this section.

Simulations with Model II - ($\kappa = A = \text{Constant}$)

A few simulations are obtained with a constant friction coefficient type of model. The bearing operates at 60 rpm and with a thrust load of 267N while the ball/race traction coefficients are held fixed at 0.015 and 0.030. The torque variations are shown in Figure 18. It is seen that both the mean torque and variations are much larger in these cases when compared with the earlier simulations. In real dimensions the mean inner race torques per ball are approximately 1.65×10^{-3} and 2.11×10^{-3} NM, respectively, for the traction coefficients of 0.015 and 0.030. For the total bearing with 24 balls, the net inner race torques will be 0.040 and 0.051 NM. These values are well within the range of experimental values shown in Figures 1 through 3.

The reason for very large torque variations with constant friction coefficient lies in the general nature of local slip variations in the ball/race contact ellipse. As shown in Figure 19, the tractive force is directly proportional to the normal load, but the direction of the tractive force is determined by the local slip vector. It is found that in the inner race contact there are two points of pure rolling (zero slip), as shown in Figure 19, and the local slip changes direction at these points. This is fairly well known phenomenon [13], but the general problem has been to determine a realistic value for the position of the pure rolling points. Since the computerized simulation of DREB allows for the general accelerations of the ball, the exact position of the pure rolling points and the resulting tractions are determined in a transient fashion and the integrations are advanced until a steady state is reached.

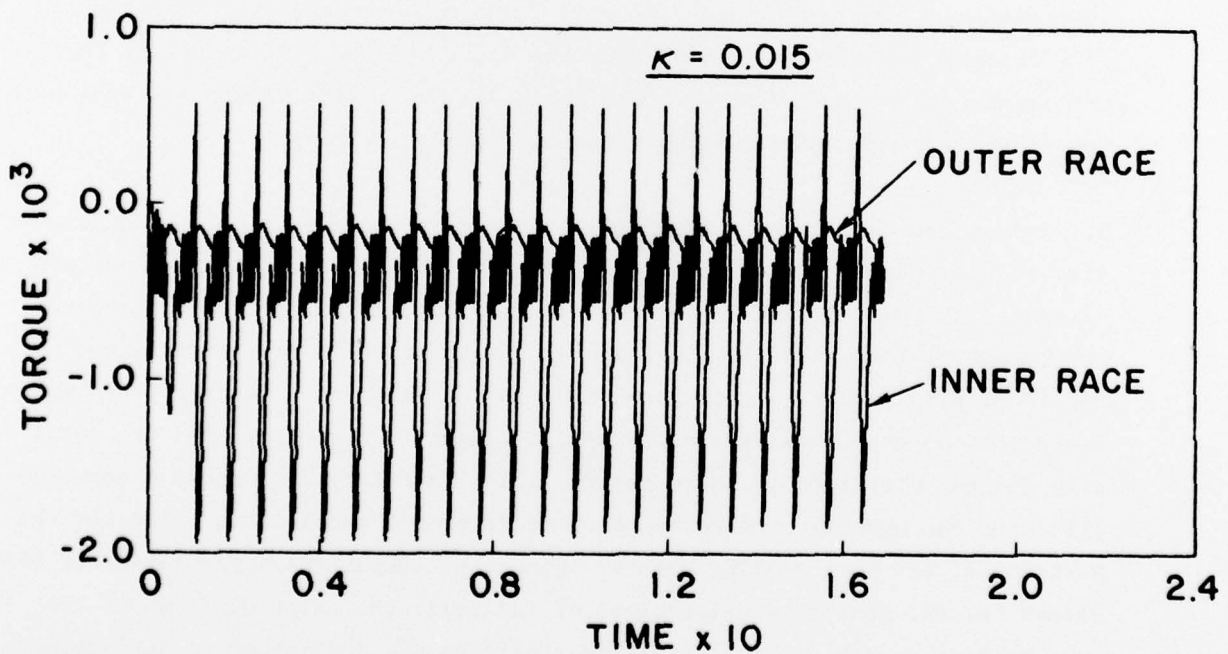
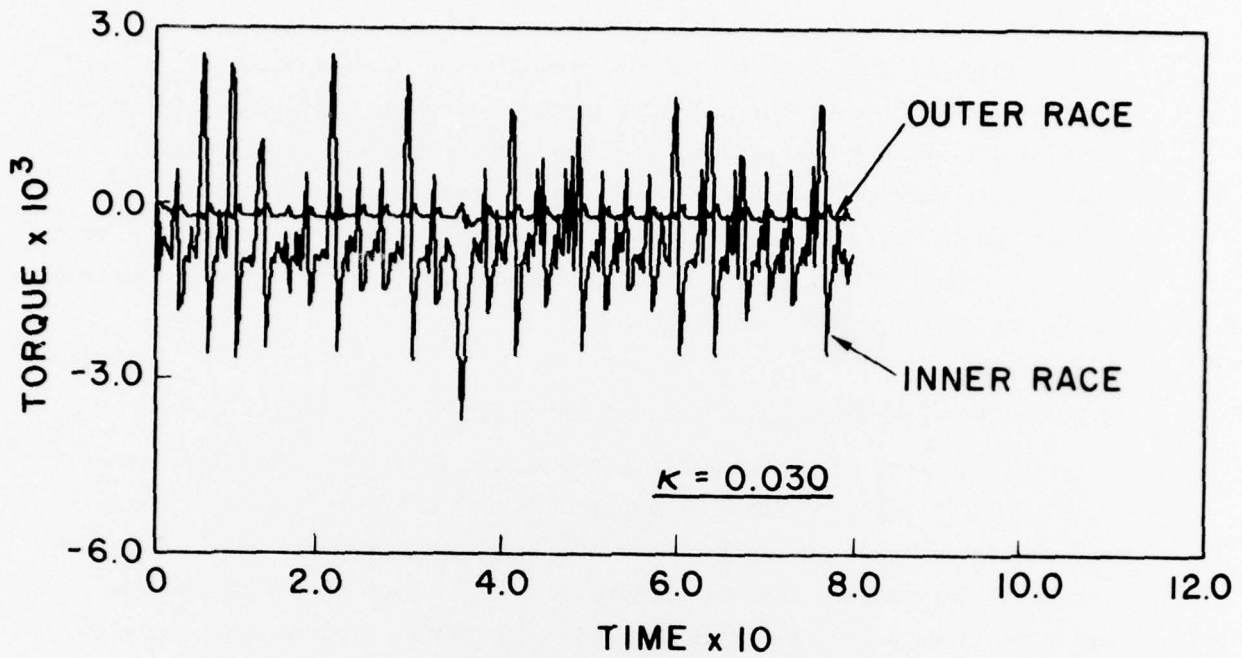


Figure 18. Variations in Torque with Constant Friction Coefficient at 267 N and 60 rpm. The torque and time scales are 2.118 NM and 6.949×10^{-4} seconds, respectively.

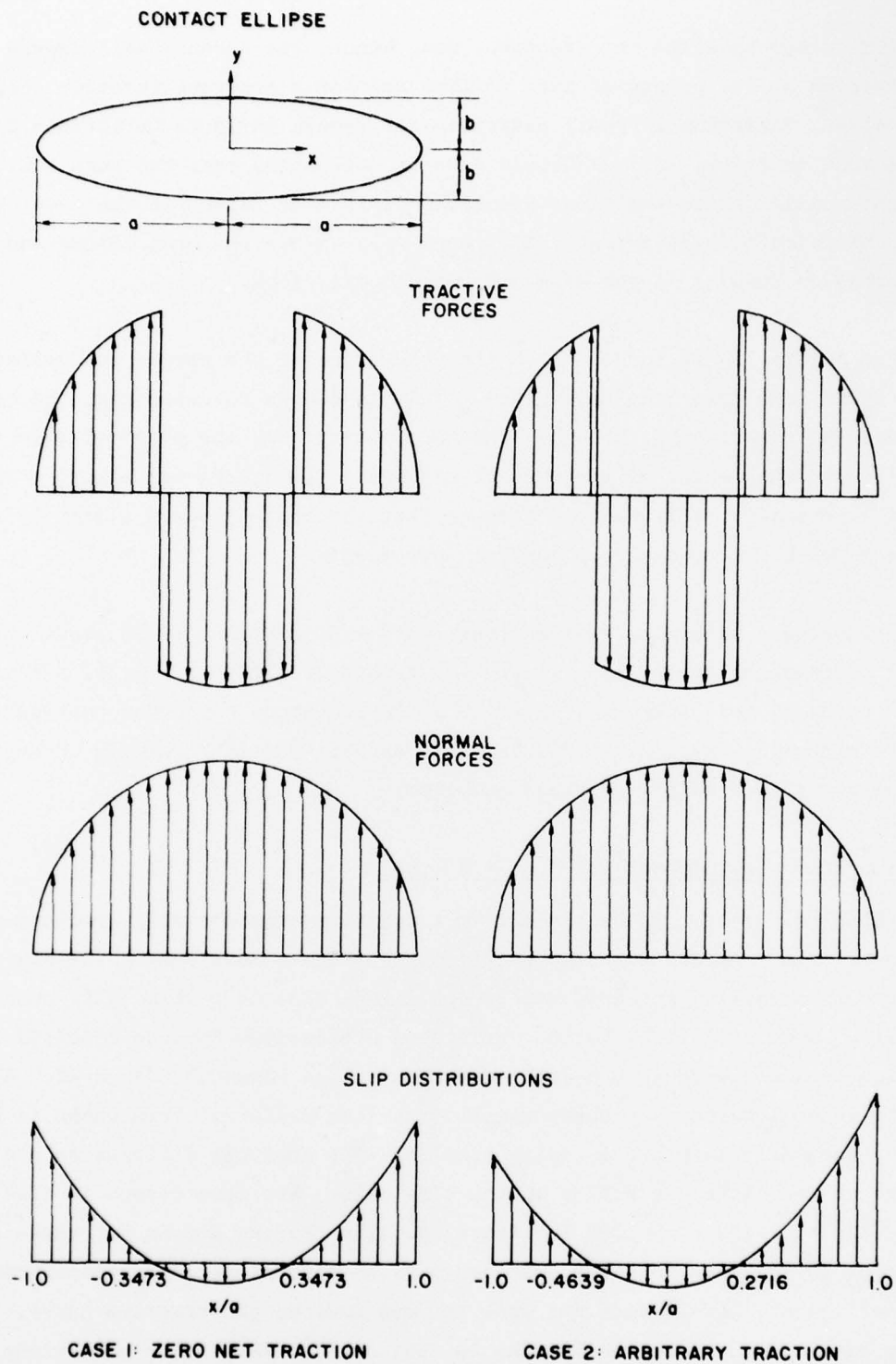


Figure 19. General Characteristics of Local Slip and Tractive Force Variations in the Ball/Race Contact Ellipse Under Constant Friction Coefficient

It is clear that the net traction, and, hence, the torque, will depend on the position of the points of pure rolling and for a constant friction coefficient, a slight variation in these positions may result in large variations in torque, as seen in Figure 18. It should also be understood that the pure rolling points continually change positions about a certain mean value, in the case of a constant friction coefficient. This mean value gives the mean torque and the variation results in the observed torque variations.

From Figure 18, it is also seen that the value of the torque and variations are very small for the outer race. This is due to the fact that the ball is spinning relative to the outer race and, therefore, the point of zero slip is close to the center of the contact ellipse. Hence, the net tractive force will be small. This basically means that the bearing works almost in accordance with the "inner race control" hypothesis.

The dominant frequency in the torque patterns of Figure 19 is about 10 kHz, and it corresponds to the elastic contact frequency [12] for the 267 N load. It is expected that there will also be a low frequency component corresponding to the kinematic frequency [12], but this is not seen in Figure 19 perhaps due to the restricted length of the simulation.

Simulations with Model III - ($\kappa = A - Bu$)

A final simulation is obtained with a negative traction slip gradient superposed on a constant traction coefficient. Such a model may be feasible with certain metallic contacts, and it could give rise to a stick-slip phenomenon [11]. Once again, the torque variations are derived for the detailed simulation obtained with this model. The results are shown in Figure 20. Although the general pattern of these results may look different from those in Figure 18, the variations are actually similar. The apparent differences are just due to the different scales on the time axis. The mean torque is also close to the one with $\kappa = 0.030$ in Figure 18. The obvious reason for these similarities is the fact that the bearing operates with almost a constant friction coefficient, and it does not want to move down on the traction curve. It may be expected that, if the bearing is subjected to large slip variations, such as those due to large radial loads, then an increased stick-slip type behavior will be seen.

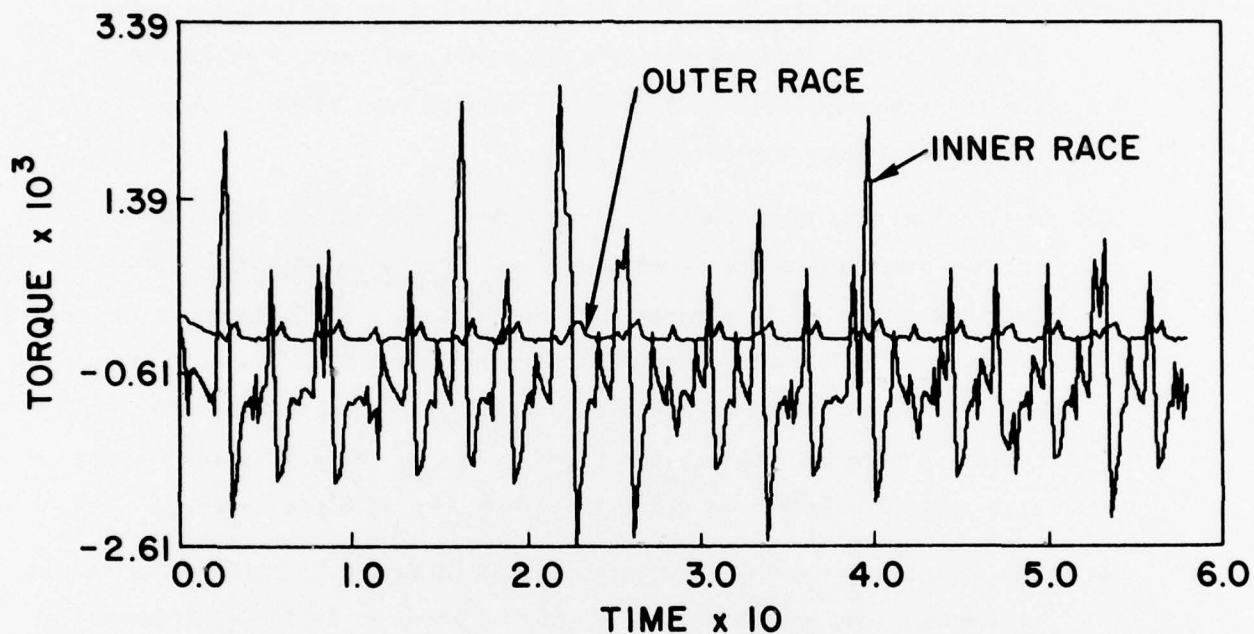


Figure 20. Torque Variations with a Negative Traction Slip Slope ($\kappa = 0.030 - 1.0$ u) at 267 N and 60 rpm. The torque and time scales are 2.118 NM and 6.949×10^{-4} seconds, respectively.

The Analytical Versus Experimental Torques

A comparison of the above analytical results with the experimental data presented in the preceding section lead to the following general findings.

- (1) Based on the validity of ball drag modelling in DREB, the general speed dependence of the observed torques is in agreement with the analytical results.
- (2) The torque predictions with constant friction coefficient are closely in range of the experimental data. In fact, by careful selection of the friction coefficient, analytical results very close to the experimental ones may be obtained.
- (3) A classical EHD type traction slope generally predicts very low torques compared to the experimental observations. In fact, for very low slips and in the range of the available EHD traction data, for a number of lubricants other than that used in the DMA bearing, the torque does not seem to depend strongly on the slope of the traction curve. A pure EHD regime, therefore, seems unlikely at least for the high-speed and high load conditions which are examined above.
- (4) The analytical results show an increased variation in torque as a result of reduced load on the bearing. This is not seen in the experimental data. However, consideration of point (5) below is essential in this regard.
- (5) Most of the frequencies observed in the torque patterns correspond to the elastic contact and kinematic frequencies [12] of the bearing, which are quite high (about 10 and 1 kHz, respectively) when compared with the range of frequencies monitored in the experimental set-up [9]. The limited length of the analytical simulations, on the other hand, does not warrant any conclusions about the presence of low frequency components in the general torque patterns.
- (6) Points (1) through (3) discussed above lead to the belief that the test bearing was operating in more of a boundary friction regime than the classical EHD regime. Or perhaps, the operation was a mixed one.

SECTION V
CONCLUSIONS

The extensive capabilities of an advanced computer program, DREB, in predicting torque in DMA bearings have been found to be realistic for the DMA bearings. Since a true traction model for the lubricant and operating conditions in the bearing is not presently available, a number of traction parameters are experimented with while obtaining the analytical simulations. After comparing these results with the experimental data, it is concluded that a constant friction coefficient type of model seems to predict more agreeable torques. The elasto-hydrodynamic models will predict much lower torques than those experimentally observed. This leads to the conclusion that the bearing operation is more in a boundary type friction or perhaps a mixed regime. The experimentally observed speed dependence of the torque is in qualitative agreement with the analytical predictions and any drag type action needs a careful attention in both the analytical and experimental simulations.

SECTION VI
RECOMMENDATIONS FOR FUTURE RESEARCH

A critical examination of the experimental torque data and the analytical results led to a number of recommendations for extended research. It is expected that the following recommendations will lead to the fulfillment of the general objectives of improved DMA bearing design and the development of a realistic analytical bearing model.

- (1) Since boundary type friction is expected in the DMA bearings, it is necessary that friction characteristics for such a contact be obtained under very slow slip velocities. A concentrated contact experiment in the range of bearing operating parameters should be performed to derive the necessary traction-slip model. Such a model will be a significant input to a realistic analytical behavior of the bearing.
- (2) Under certain conditions the bearing can operate in the elasto-hydrodynamic (EHD) regime and, hence, the formulation of a realistic EHD traction model is essential in order to predict bearing torque under such conditions. The EHD traction model can be readily derived from the conventional rolling disc type of concentrated rolling/sliding contact experiments. The experiments will once again be performed in the range of the operating parameters of a typical DMA bearing.
- (3) For purely thrust loaded applications the question of a successful operation of a full complement (cageless) bearing is still open and most questions are directed toward the collision of counter rotating balls under imperfect geometrical and/or operating conditions. It will, therefore, be helpful to extend the capabilities of DREB to include such collisions. A systematic sensitivity type analytical investigation may then be undertaken to investigate the feasibility of such a bearing.
- (4) For the purpose of improving the predictive strength of an analytical model, such as DREB, it may be very helpful if a few experiments are run in the EHD regime with a lubricant for which a traction model has already been obtained. A MIL-L-7808 type oil will be a good candidate for such an investigation.

- (5) Several improvements in the present apparatus for instrumenting DMA bearings are essential. The primary factors requiring attention are the torque measuring device and its mounting on the inner race. Unlike the present set-up, any motion of the inner race must be avoided. Another recommended improvement concerns the high frequency responses. The elastic contact and kinematic frequencies have been found in all the analytical simulations, confirming their presence in the experimental data will add to the valid comparisons between the predicted and observed behavior. Some accelerometers can be mounted on the inner race, and also the torque data can be processed by the conventional spectral analyzers and most of the high frequency content can be measured.
- (6) Electrical resistivity type measurements will be helpful in establishing the extent of metal contact in typical bearings. This can be easily done by surface interaction measurement devices such as an Asperitac*.

*An instrument made by MTI to measure the electrical contact resistance variations between sliding surfaces.

REFERENCES

1. Jones, A. B., "Ball Motion and Sliding Friction in Ball Bearings", J. Basic Engg., ASME Trans., March 1959. pp. 1-12.
2. Jones, A. B., "A General Theory for Elastically Constrained Ball and Radial Roller Bearings Under Arbitrary Load and Speed Conditions", J. Basic Engg., ASME Trans., June 1960, pp. 309-320.
3. Harris, T. A., ROLLING BEARING ANALYSIS, Wiley, 1966.
4. Walters, C. T., "The Dynamics of Ball Bearings", J. Lub. Tech., ASME Trans., Vol. 93F, 1971, pp. 1-10.
5. Gupta, P. K., "Transient Ball Motion and Skid in Ball Bearings", J. Lub. Tech., ASME Trans., Vol. 97F, 1975, pp. 261-269.
6. Gupta, P. K., "Dynamics of Rolling Element Bearing (DREB) Computer Program", A program developed at MTI.
7. Rivera, M. P., "Short Time Torque Investigations on DMA-Bearings", ASME Paper #76-Lub-20 presented at the ASME/ASLE Lub. Conf., Boston, October 5-7, 1976. To be published in J. Lub. Tech., ASME Trans.
8. Tyler, J. C., Carper, H. J., Brown, R. D., and Ku, P. M., "Analysis of Film Thickness Effect in Slow-Speed Lightly Loaded Elastohydrodynamic Contact - Part I: Development of Film Thickness Measurement Technique", Technical Report AFML-TR-74-189, Part I, December 1974, Wright Patterson Air Force Base, Ohio, Prepared by Southwest Research Institute, San Antonio, Texas, under contract No. F33615-73-C-5123.
9. Rivera, M. P., Personal Communications.
10. Schlichting, H., BOUNDARY LAYER THEORY, McGraw Hill, 1968.
11. Rabinowicz, E., FRICTION AND WEAR OF MATERIALS, Wiley, 1965.
12. Gupta, P. K., Winn, L. W., and Wilcock, D. F., "Vibrational Characteristics of Ball Bearings", J. Lub. Tech., ASME Trans., Vol. 99F, 1977, pp. 284-289.
13. Bisson, E. E., and Anderson, W. J., ADVANCED BEARING TECHNOLOGY, National Aeronautics and Space Administration Publication, NASA SP-38, 1965.